

INFLUENCE OF STRENGTH ON THE FRACTURE ENERGY OF HPC

B.K. Raghu Prasad*, G. Appa Rao** and R. Patnaik***

* Professor, ** Research Scholar, Department of Civil Engineering, Indian Institute of Science, Bangalore-560 012, India.

** (Also) Assistant Professor, Department of Civil Engineering, Sri Venkateswara University, Tirupati-517 502, AP, India.

*** Additional Chief Engineer, A&CED, BARC, Mumbai-400 085, India.

ABSTRACT

An experimental investigation of the influence of various parameters on the strength and fracture behavior of HPC is reported. Three-point bend beam specimens of size 100mmx150mmx1000mm were adopted with notch-to-depth ratio 0.5 in all the test specimens. In this study a wide range of concrete mixes have been designed to vary the strength of concrete. Two parameters were adopted to change the properties of concrete. Silica fume was used at 10, 15, and 20 percent as cement replacement material by weight of binder. At each silica fume content, three different water-binder ratios 0.29, 0.32 and 0.34 were adopted. It has been observed that the workability of fresh concrete was good and it was easily flowing with the addition of high-range water reducing agent. Changing the silica fume content from 10 % to 20 % showed hardly any influence on the compressive strength at lower water-binder ratios. However, the highest strength has been achieved at 15 % silica fume with 0.32 water-binder ratio. The fracture energy of HSC decreases as the water-binder ratio increases with 10 % and 15 % silica fume contents. The fracture energy seems to be slightly highest at 20 % silica fume content at water-binder ratio 0.32. The fracture energy and the corresponding characteristic length seem to increase as the compressive strength of concrete increases. Ductility factor increases as the w/b ratio increases, while it decreases with silica fume up to 15 %, beyond which it increases. The fracture energy increases as the compressive strength increases. It has also been observed that the softening response was good in all the concrete mixes. However, the softening response was gradual in relatively low strength concrete.

Keywords: Characteristic length, Ductility factor, Fracture energy, High-strength concrete, Silica fume content.

INTRODUCTION

High strength concrete may be considered as relatively a new material. The use of silica fume, fly ash and superplasticizers with careful selection of constituent materials has made the production of HSC easier and more economical. During the last decade, most of the research has been concerned with increasing the strength of HSC. It behaves more like a brittle material and the post peak response seems to be very steep (1). However, the research was lacking in understanding the fracture behavior of HSC. Very few research efforts have been made to quantify the fracture behavior of HSC. The fracture energy, G_F is one of the important material properties for the design of concrete structures. For the fictitious crack model (FCM) by Hillerborg and Co-workers (6,7,8) the fracture energy, G_F , tensile strength f_t , and the stress-CMOD relationship completely describe the fracture characteristics of concrete. The RILEM-50 TMC (18,19) recommended a simple method for the determination of G_F using simple three-point bend beam specimens. Nevertheless, the fracture energy, G_F and fracture toughness, K_{Ic} depend upon the size and geometry of the test specimen. To overcome this drawback, Petersson (12) proposed a direct method independent of specimen size and notch depth, where in the fracture energy, G_F defined as the area under the load-deflection curve per unit fractured surface area is used to characterize the process of fracture. Based on the results of the fracture energy G_F of mortar and concrete, obtained from about 700 beam tests, Hillerborg (9) concluded that there is a tendency for G_F to increase when the maximum aggregate size increases from 8 mm to 20 mm. Walsh (24), and Bazant and Oh (2) also reported the same tendency with the aggregate size. However, Petersson (13) reported that the fracture energy does not seem to be affected by the maximum particle size, while l_{ch} increases with increasing maximum particle size.

The fracture surfaces are smooth and less tortuous in high-strength concretes with silica fume (20). The fracture energy decreases and the brittleness index increases significantly with the incorporation of large size aggregate (21). But Zhou et al. (27) reported that the fracture energy increases with increasing aggregate size and stiffness, and the K_{Ic} increases with increasing compressive strength. The type and size of coarse aggregate has also influenced the characteristic length, l_{ch} of concrete. It decreases with the increase in the compressive strength and the type of fine aggregate has no influence on the fracture energy of concrete (10). Giaccio et al. (5) reported that the fracture energy, G_F , of concrete increases with increase in the size of aggregate and strength of concrete, the displacements at peak load depend on the type and size of aggregate and the characteristic length decreases as the concrete strength increases. Barr et al. (3,4) reported that the fracture toughness obtained on beam specimens were independent of the size of coarse aggregate. But using the compact tension specimens, the highest toughness values were observed with 10 mm aggregate and the lowest with 20 mm aggregates. Therefore it appears that even till to date, the influence of the maximum size of the aggregate has not been clearly understood, much less in

concretes of high strength. Furthermore, the influence of silica fume, water-cement ratio and other mix proportions has been reported (11,14,23,25).

EXPERIMENTAL PROGRAM

Materials

Commercially available 43 grade ordinary Portland cement was used for the program. The influence of silica fume and water-binder ratio was studied on the mechanical and fracture properties of HSC, in which cement was replaced partially by silica fume at 10, 15 and 20 percent by weight of binder. For every silica fume content, the water-binder ratio was varied. The proportioning of cementitious material (cement + silica fume), sand and coarse aggregate were kept constant throughout the program. Table 1 shows the mix details and various quantities of constituent materials. Silica fume ($\text{SiO}_2 = 93.6\%$) was used at 10, 15 and 20 percent by weight of binder as partial replacement material to study the influence of silica fume on various properties of concrete. Sand was natural river sand passing through 2.36 mm sieve. Specific gravity of the sand was 2.65 and its bulk density was 1580 kg/m^3 . Fineness modulus of the sand was 2.83. Coarse aggregate was crushed white granite containing different sizes of aggregate particles with maximum size of 20 mm. The specific gravity and fineness modulus were 2.60 and 6.84 respectively. Potable water was used for both mixing the concrete and curing the test specimens. The influence of water-binder ratio on the behavior and various properties of HSC was studied. Three water-binder ratios namely 0.29, 0.32 and 0.375 were adopted. High range water reducing agent (HRWRA) was used to improve the workability of the fresh concrete. The HRWRA was thoroughly mixed with water before pouring in to the uniformly mixed dry concrete. Table 1 shows the quantities of the constituent materials of the concretes used for the program. The mix proportions of the concrete mixes were: C : FA : CA : 1 : 1.29 : 2.14. The water content was varied in the concrete mixes to study its influence on the fracture properties of concrete.

Table 1: Mix Proportioning and Quantities of Constituent materials in the various concretes

Mix Designation	Cement (kg/m^3)	Silica Fume		Water Content (lit/m^3)	Sand Content (kg/m^3)	Coarse Aggregate Content (kg/m^3)	W/B ratio
		%	Content (kg/m^3)				
HSC-A-10	459	10	51	148	659	1092	0.29
HSC-A-15	433.5	15	76.5	148	659	1092	0.29
HSC-A-20	408	20	102	148	659	1092	0.29
HSC-B-10	459	10	51	163	659	1092	0.32
HSC-B-15	433.5	15	76.5	163	659	1092	0.32
HSC-B-20	408	20	102	163	659	1092	0.32
HSC-C-10	459	10	51	191	659	1092	0.375
HSC-C-15	433.5	15	76.5	191	659	1092	0.375
HSC-C-20	408	20	102	191	659	1092	0.375

W = Water, B = Binder (cement + silica fume)

DIMENSIONS AND PREPARATION OF THE TEST SPECIMENS

Three-point bend (TPB) beam specimens were adopted with central notches made as per the RILEM-TMC 50 recommendations. The notch-to-depth ratio was 0.5. The sizes of the test specimens were; 100 mm x 150 mm x 1000 mm with an effective length of 750 mm. All the constituent materials of the concrete were mixed thoroughly in the dry state. The water with HRWRA was mixed with concrete in three stages; at every stage water was added and mixed until the mix was uniform. Table vibrator was used for compacting of the concrete in the moulds. The test specimens were prepared using steel channel sections placed back to back with the required geometric dimensions. Two beams were tested for each concrete mix. After 24 hours, the test specimens were stripped off from the moulds and subsequently kept for curing in water for 28 days. The environmental climatic conditions were as follows: temperature of $25 \pm 2^\circ \text{C}$ and relative humidity of 70 %. The notch was formed using diamond saw cut after about 28 days of casting of the test specimens.

TESTING OF SPECIMENS

The three-point bend beam specimens were tested under loading control machine. To obtain the post-peak response of the TPB under load control, The testing machine was carefully operated. The load was increased in a constant rate up to the ultimate load. The point where the ultimate load is likely to attain in the specimen could be identified by the slow movement of the load indicator needle at which micro cracking has been initiated to widen. The micro cracking extension has been generally initiated at about 90 percent of the peak. The extension of the micro cracking could be observed by very quick changes in the LVDT reading. In order to achieve stable crack growth and post peak softening response of concrete, the pressure volve was closed partially to avoid sudden dropping down of the load after peak. When the load indicator was started to come back just after the peak, then the pressure volve was slowly opened to achieve stable softening response. The whole process of loading the specimens was completed in about 6 to 8 minutes. The load was increased at a constant rate at different load increments. At every load increment, using linearly variable differential transducer (LVDT) fixed at the crack mouth in the test specimen monitored the variation of crack mouth opening displacement (CMOD). The variation of load with CMOD was used to evaluate the work of fracture and hence the fracture energy. Hillerborg (9) reported the results of fracture energy of concrete on 700 beams tested in 14 laboratories. It has been reported that stable post-peak response should be observed using displacement/CMOD control, but with stiff machine. However, the results from various laboratories show that the stable crack growth could be achieved even in the ordinarily equipped laboratories. In this program load was carefully controlled and it was possible to achieve the stable post-peak response in HSC. Two specimens were tested for each concrete mix and the average values of the results are reported. The compressive strength (f_c) of concrete was determined on 100 mm cubes at the age of 28 days. The tensile strength and modulus of elasticity have been evaluated by the following equations (Eq. 1 and Eq. 2) proposed by Rao and Raghu Prasad (16):

$$f_t = 0.5\sqrt{f_c} \dots\dots\dots(1)$$

$$E = 4680\sqrt{f_c} \dots\dots\dots(2)$$

DETERMINATION OF FRACTURE ENERGY, G_F

Earlier, the fracture energy has been reported from the TPB specimens from Load vs. Load point displacement variations. However, various errors have been reported in the literature while estimating the fracture energy, using Load vs. Load point displacement variations. The errors included are: crushing of supports and load points, significant dissipation of energy in the bulk of concrete under highly stressed zones, which led to adopt a new technique based on Load vs. CMOD variations. Now, the fracture energy is calculated by the work of fracture divided by the area of uncracked ligament in the TPB. Though the area under the Load-CMOD variations seems to be lower than that of the one with Load vs. Load point displacement, the fracture energy seems to be free from the above mentioned experimental errors and may be considered as the true fracture energy. The fracture energy is the energy required for creating unit area of crack surface. It is calculated as the work of fracture divided by the area of the uncracked ligament.

$$G_F = \frac{W_F}{b(d - a_0)} \dots\dots\dots(3)$$

Where G_F is the fracture energy, W_F is the work of fracture, d is the depth of the beam, b is the width and a_0 is the notch depth.

TEST RESULTS AND DISCUSSION

Variation of Compressive Strength

The variation of compressive strength of concrete with w/b ratio is shown in Fig. 1. In all the concretes, in general, higher values of the compressive strengths have been observed with w/b ratio 0.32. The compressive strength seems to decrease as the w/b ratio increases beyond 0.32. Fig. 2 shows the variation of compressive strength with silica fume content at different w/b ratios. At w/b ratio 0.32, the compressive strength of concrete seemed to be higher than those did with 0.29 and 0.375 w/b ratios. Further, the compressive strength of concrete seems to show higher values with silica fume contents between 10

% and 15 %. Beyond 15 % silica fume content, compressive strength of concrete decreases at 0.32 w/b ratio. However, in the case of concretes at different silica fume contents at 0.29 w/b ratio, the compressive strength has been almost the same in all the concretes. That means, at a water-binder ratio 0.29, changing the silica fume content from 10 % to 20 % seemed to show hardly any influence by the silica fume. But at 0.32 w/b ratio, the higher value of compressive strength has been observed at 20 % silica fume. It has been apparent from the behavior of the concretes with different silica fume content with different water-binder ratios that the presence of higher contents of silica fume requires more water for complete reaction. Zhou et al. (27) reported that changing silica fume content from 10 % to 15 % does not affect the compressive strength of concrete for a water-binder ratio 0.23. However, a small increase in compressive strength has been observed for a water-binder ratio 0.32. Further, silica fume makes a greater contribution in enhancing the strength of low strength concrete than HSC. Therefore, silica fume content may be reduced when producing concretes with lower water-binder ratio. However, Sabir (21) reported that silica fume replacements up to 28 % had beneficial effect on the compressive strength with the water-binder ratios 0.35 and 0.40. It may be stated at this juncture that different combinations of silica fume and water contents results in different strength levels. However, use of higher water contents produce better strengths with higher silica fume contents. The optimum silica fume content seems to range between 15 % and 20 % for producing higher compressive strength (26).

Variation of Fracture Energy

Fig. 3 shows the variation of fracture energy with water-binder ratio in HSC. It demonstrates that in concretes containing silica fume contents 10 % and 15 %, the fracture energy decreases as the water-binder ratio increases. However, the concrete incorporated with 20 % silica fume exhibited highest value of fracture energy at w/b ratio 0.32. At w/b ratio 0.29, the concrete with 20 % silica fume achieved lower fracture energy. At w/b ratio 0.375, the fracture energy seems to be higher at 20 % silica fume content. It has been very clear that the fracture energy of concrete decreases as the w/b ratio increases at lower silica fume contents. At higher silica fume contents, it demands for more water due to increase in the specific surface area of silica fume for complete reaction and continuous hydration of cement. At a particular silica fume content, concretes may exhibit optimum fracture energy at a particular water-binder ratio. In the case of concretes containing 20 % silica fume, the highest value of fracture energy has been observed with w/b ratio 0.32. Surprisingly, Zhou et al. (27) reported that the fracture energy of concrete with 20 mm coarse aggregate increases as the water-binder ratio decreases with silica fume contents of 10 % and 15 %. However, in the case concrete with 10 mm aggregate, the fracture energy decreases as the water-binder ratio changes from 0.32 to 0.23. In the present program, the maximum size of coarse aggregate was 20 mm. The fracture energy of concrete decreases as the water-binder ratio increases with 10 % and 15 % silica fume. However, with 20 % silica fume content, lower fracture energy has been observed at the water-binder ratio of 0.29. This may be due to insufficient amount of water available for the complete hydration of cement in the concrete. Wittman et al. (25), however, reported that the fracture energy increases as the maximum size of coarse aggregate increases, but it slightly decreases as the water-cement ratio increases in plain cement concretes at w/c ratios 0.43, 0.5 and 0.60. Nallathambi et al. (11) reported that the toughness of concrete decreases significantly as the water-cement ratio increases. The water-cement ratios were 0.5, 0.55, 0.60 and 0.65. The decrease in the fracture toughness with increased water-cement ratio reflects the decrease in the compressive strength of the concrete. Philips and Binsheng (14) also reported that the fracture energy decreases as the water-cement ratio increases. The energy dissipated owing to irrecoverable deformation contributes a large share of the whole work done by the external force. It is worth to point out at this juncture that in HSC, major fraction of the dissipated energy is utilized for breaking the bond due to surface forces in the concrete. While the fraction of fracture energy dissipated for overcoming the micro cracking and fracture process is generally very negligible. The type of fracture surfaces in HSC shows that the crack profile is relatively straight with less tortuosity in which crack traveled through the aggregate particles. Pulling out of the coarse aggregate particles has been pronounced very less with increase in the strength of HSC.

Fig. 4 shows the variation of fracture energy with silica fume content at different w/b ratios in HSC. It has been noticed that the fracture energy seems to be slightly higher at 15 % silica fume at 0.29 w/b ratio. As the w/b ratio increased further, 0.32 and 0.375, the fracture energy seemed to increase with silica fume content beyond 15 %. Nevertheless, the concrete with 20 % silica fume at 0.32 w/b ratio exhibited highest fracture energy. This could be due mainly to the non-evaporable water content that will enable continuous pozzolanic reaction of silica fume at lower strength development with age. In other words, the silica fume reacts quickly at lower w/b ratios during the initial hydration period. As the w/b ratio increases, the hydration continuous with the presence of non-evaporable water content with higher silica fume contents at slower rate.

Rao and Raghu Prasad (15) reported that the fracture energy increases with the maximum size of coarse aggregate with single sized aggregate, but the increase has been observed to be very significant with the combination of different sizes of coarse aggregate sizes. However, the fracture energy in HSC has been higher with silica fume (10 %, w/b = 0.325). In high-strength concrete, the total energy may be considered in two forms. The first form of energy seemed to be utilized for overcoming the surface forces of concrete (surface energy), while the second form for overcoming the cohesive forces due to aggregate bridging, aggregate interlocking, friction forces and other mechanisms in the fracture process zone. The interface between cement paste and aggregate has been very strong, impermeable and dense. The post-peak response seems to be steep

with increase in the strength of concrete. This process results in the catastrophic behavior of high-strength concrete. Due to strong interface, the process zone in front of the initial crack tip localizes resulting in the decrease in the absorption of fracture energy in this zone. With the addition of silica fume, the strength of hardened cement paste and aggregate-matrix interface increases with age of concrete. The fracture energy decreases with silica fume resulting in high brittleness index (22,23). Smoother fracture surfaces have been noticed with silica fume (20). But Barr et al. (3,4) reported different variations of test results from their studies on the influence of coarse aggregate on fracture energy and fracture toughness of concrete with different types of specimens. Fig. 5 shows the variation of fracture energy with compressive strength of HSC. It shows that the fracture energy increases as the compressive strength of concrete increases. This is true to the fact that the bond strength in HSC is generally high and micro cracking decreases as the strength increases due to high impermeable structure of HSC. In the case of HSC, the major part of the fracture energy has been dissipated for overcoming the surface forces.

Variation of Characteristic length

Brittleness of concrete or otherwise ductility is measured also by a parameter called characteristic length, l_{ch} . Fig. 6 shows the variation of characteristic length, proposed by Hillerborg ($l_{ch} = EG_F/f_c^2$) and modified by Rao and Raghu Prasad (17) ($l_{ch} = EG_F/f_c f_c$), with the compressive strength of concrete. It has been observed that the characteristic length, calculated by Hillerborg's expression, ranged between 150 and 300 mm. In high strength concrete, the influence of compressive strength could be very significant. It cannot be neglected while evaluating the fracture process zone. That means the concrete might behave in a brittle manner when the strength of concrete increases. It has been observed that the characteristic length of concrete increases as the maximum size of coarse aggregate increases. Tasdemir et al. (22,23) reported similar conclusions for concrete mixes with silica fume. It has been observed that the characteristic length of concrete increases slightly with silica fume. The crack surfaces are less tortuous with silica fume. It has been also reported that in high strength concrete, the characteristic length values are two to three times smaller than those obtained in conventional concrete (5). The characteristic length of concrete decreases as the strength increases (10,27). It is quite early to conclude that a mere decrease or increase in the characteristic length signifies brittleness or ductility of concrete respectively, which means that the expression for the characteristic length should be further modified for HSC.

Variation of Ductility Factor

Ductility of concrete can be defined in terms of deformation, rotation and now in terms of CMOD. It is defined as the ratio of deformation/deflection/rotation or CMOD at the failure to the one at the yield point. The ratio of the CMOD at failure to the CMOD at the yield point is defined as the ductility factor of concrete in TPB central notched beam specimens. It is very hard to distinguish the exact yield point in concrete due to its non-linear load-CMOD variations. However, for the present program the yield point has been assumed at the point where linearity tends to change to non-linear. The linearity of the load-CMOD could be observed up to about 85 to 90 percent of the peak load in HSC. The point where linearity ceases to non-linearity, it is generally assumed that the micro cracking extension has been initiated.

$$Ductility \dots Factor = \frac{(CMOD)_{Failure}}{(CMOD)_{Yield}} \dots \dots \dots (4)$$

Fig. 7 shows the variation of ductility factor with w/b ratio in HSC. It has been noticed that the ductility factor decreases with w/b ratio up to about 0.35, thereafter it has been in the increasing trend with 15 % silica fume. However, in concretes with 10 and 20 % silica fume contents, it increases as the w/b ratio increases. But the rate of increase seems to be high with 10 % silica fume. As has been seen in Fig. 8, the variation of ductility factor with silica fume content, the ductility factor increases up to 15 % silica fume, thereafter it decreases with silica fume at w/b ratio of 0.29. However, different trend has been observed in concretes with w/b ratios of 0.32 and 0.375. The ductility factor decreases as the silica fume content increases up to about 16 %, there after, it slightly increases with silica fume content.

Softening Response in HSC

The load-CMOD variations are linear up to about 90 percent of the ultimate load, beyond which microcracking has started. This has been indicated by nonlinear variation up to the peak load. This indicates that the microcracking in front of the crack tip seems to be very limited and the size of fracture process zone is likely to be small in HSC. The post peak response seems to be gradual, which depends up on the type of concrete mix. Figs. 9 to 11 show the softening of concrete in concrete mixes with 0.29, 0.32 and 0.375 water-binder ratios respectively using different silica fume contents. From the experimental observations, it could be possible to obtain good softening behavior using stable three-point bend specimens with less stiff machines with ordinary equipment on small beam specimens.

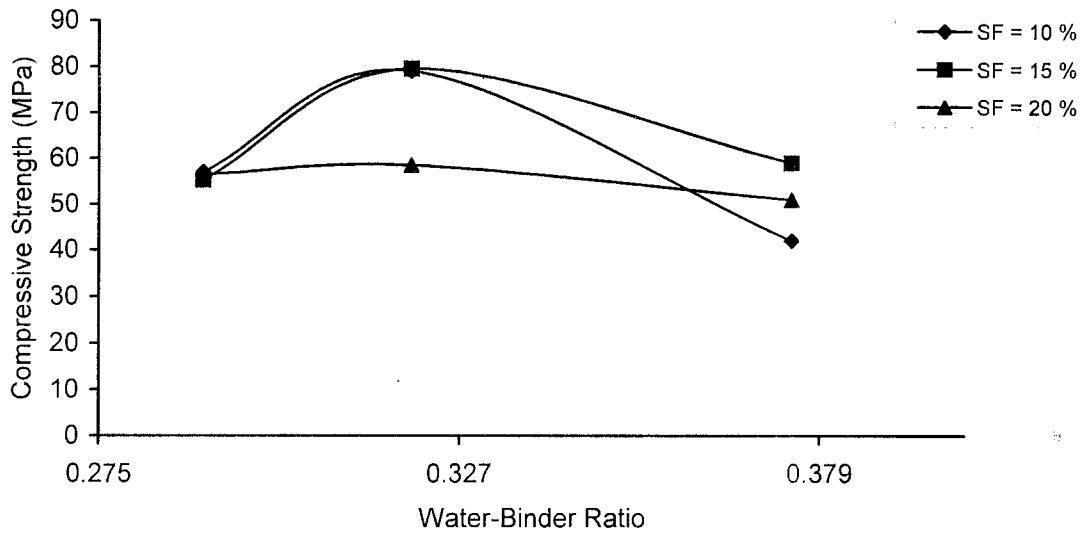


Fig. 1: Variation of compressive strength with water-binder ratio in HSC.

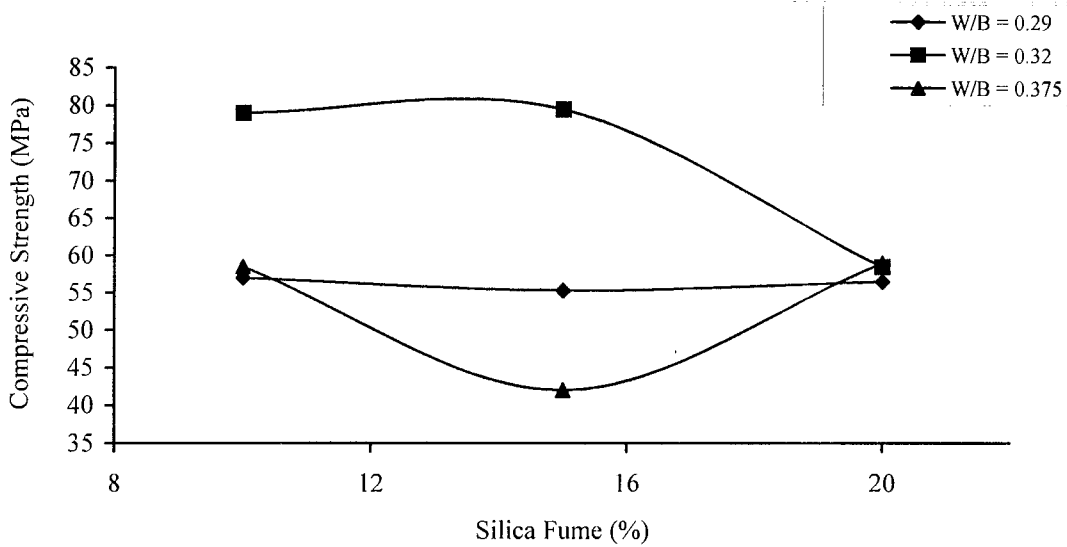


Fig. 2: Variation of compressive strength of HSC with silica fume at different w/b ratios.

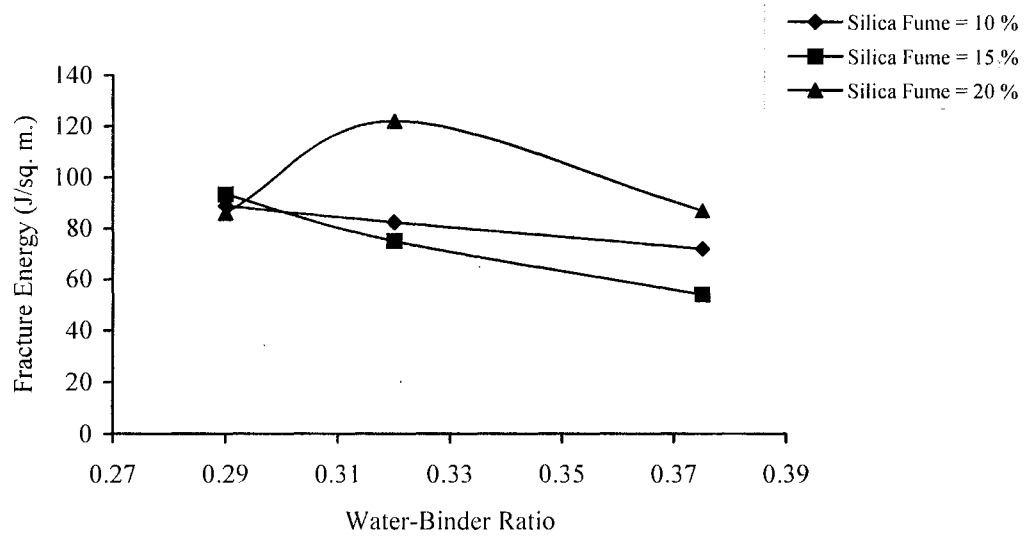


Fig. 3: Variation of fracture energy with water-binder ratio in HSC with different silica fume contents.

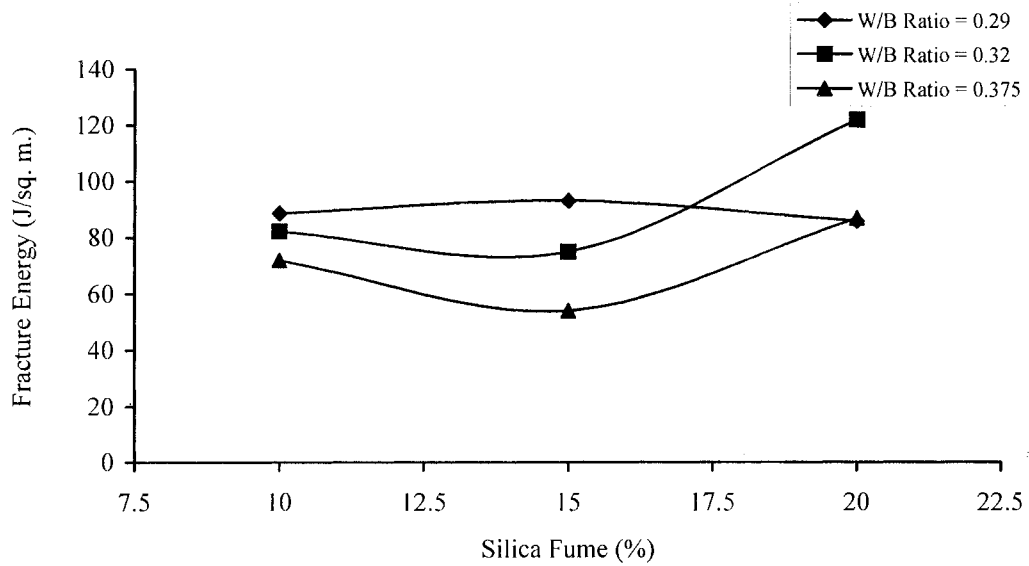


Fig. 4: Variation of fracture energy with silica fume content in HSC at different water-binder ratios.

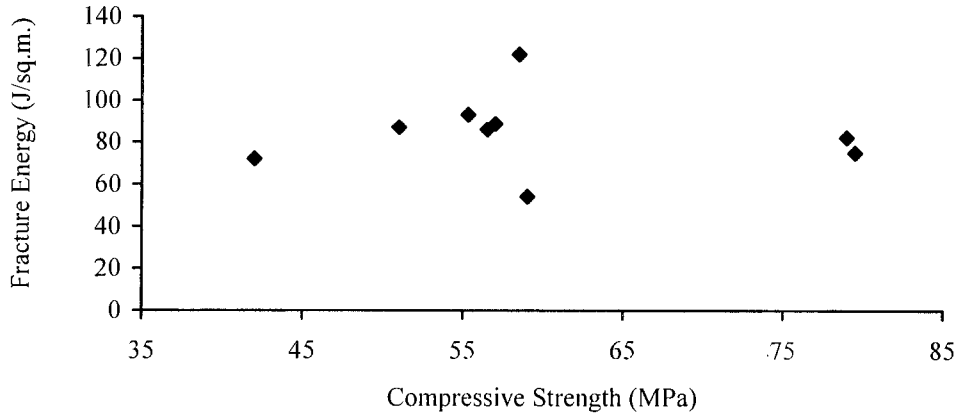


Fig.5: Variation of fracture energy with compressive strength of HSC with different silica fume contents at different w/b ratios.

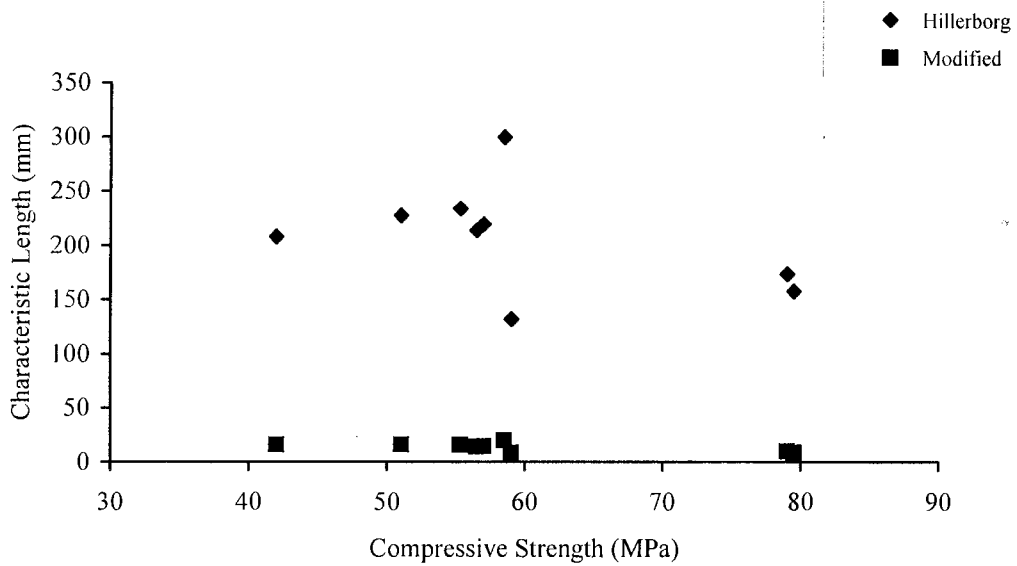


Fig.6: Variation of characteristic length with compressive strength in HSC.

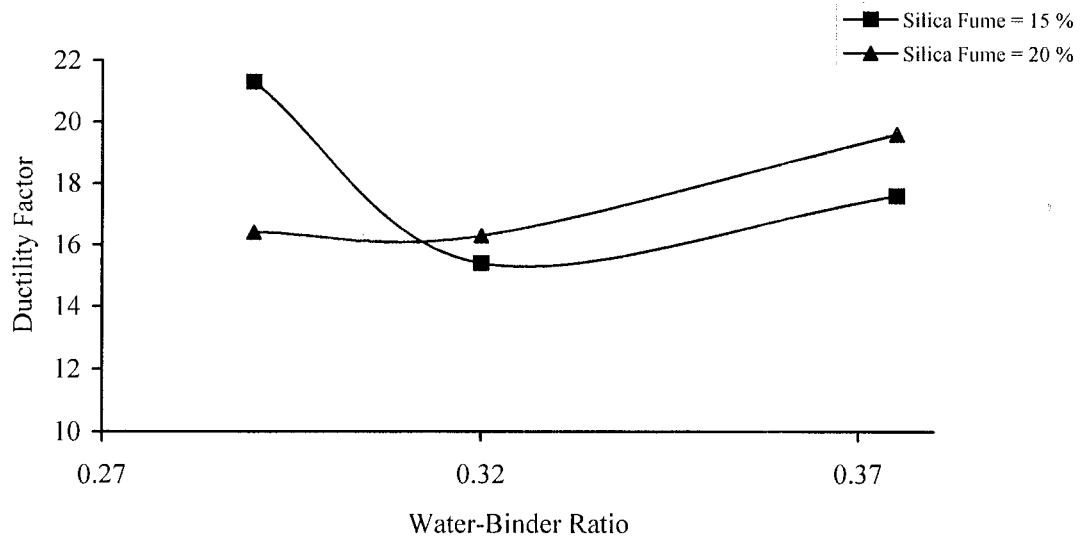


Fig. 7: Variation of ductility factor in HSC with water-binder ratio.

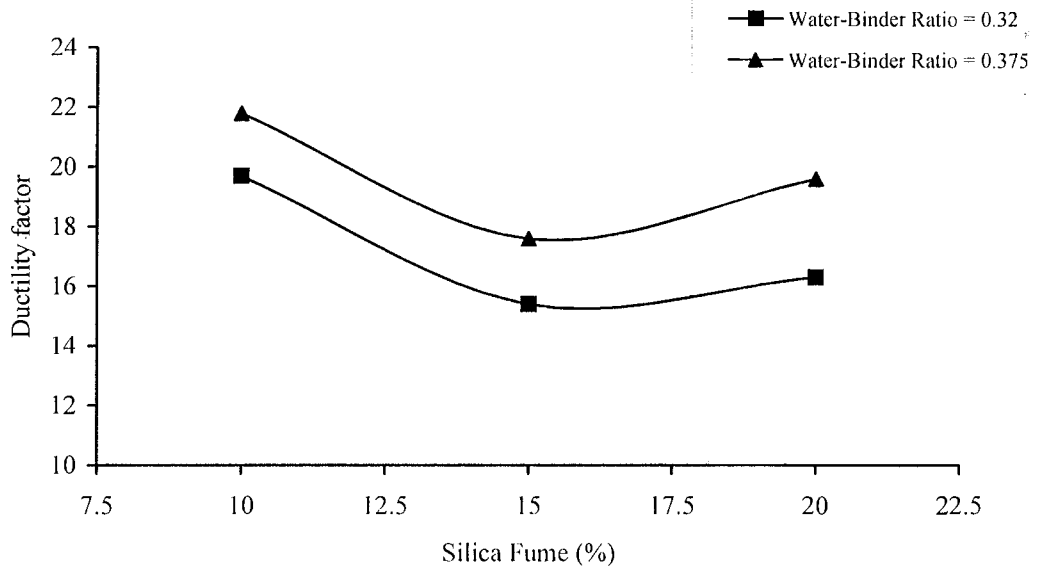


Fig. 8: Variation of ductility factor with silica fume content in HSC.

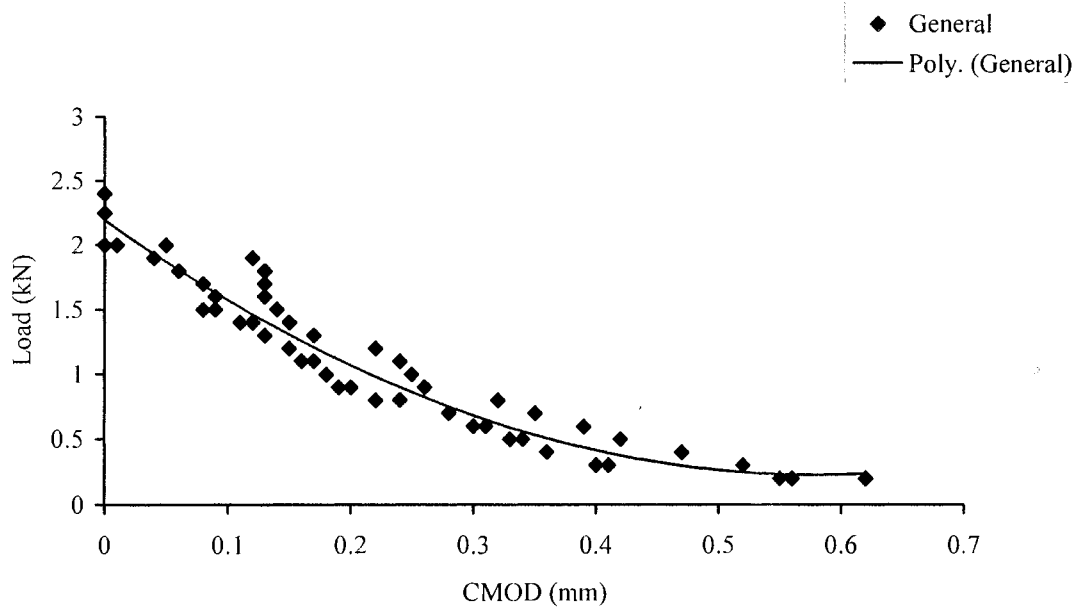


Fig. 9: General softening curve in HSC with $w/b = 0.29$.

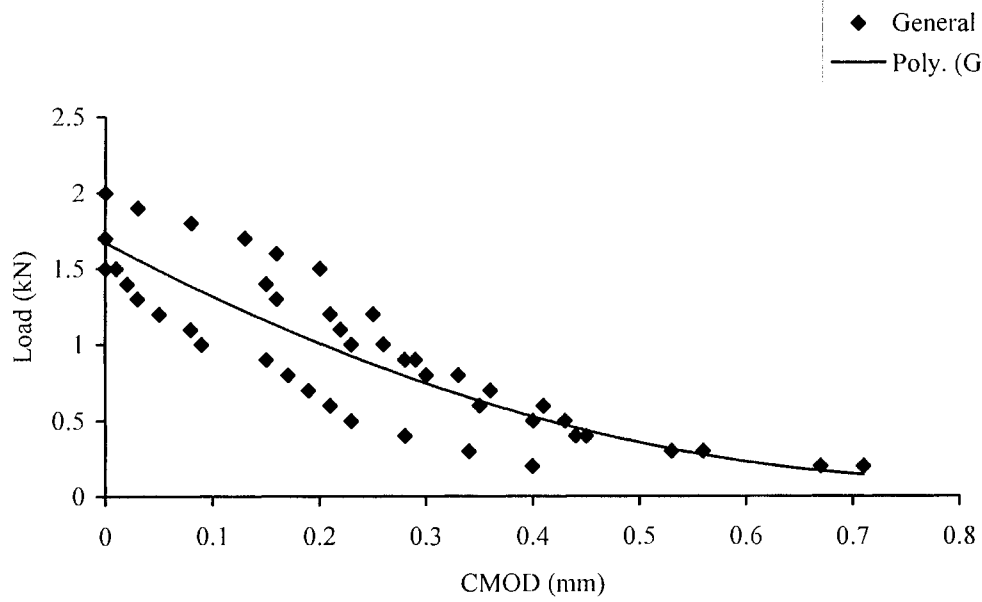


Fig. 10: General softening curve in HSC with w/b ratio = 0.32.

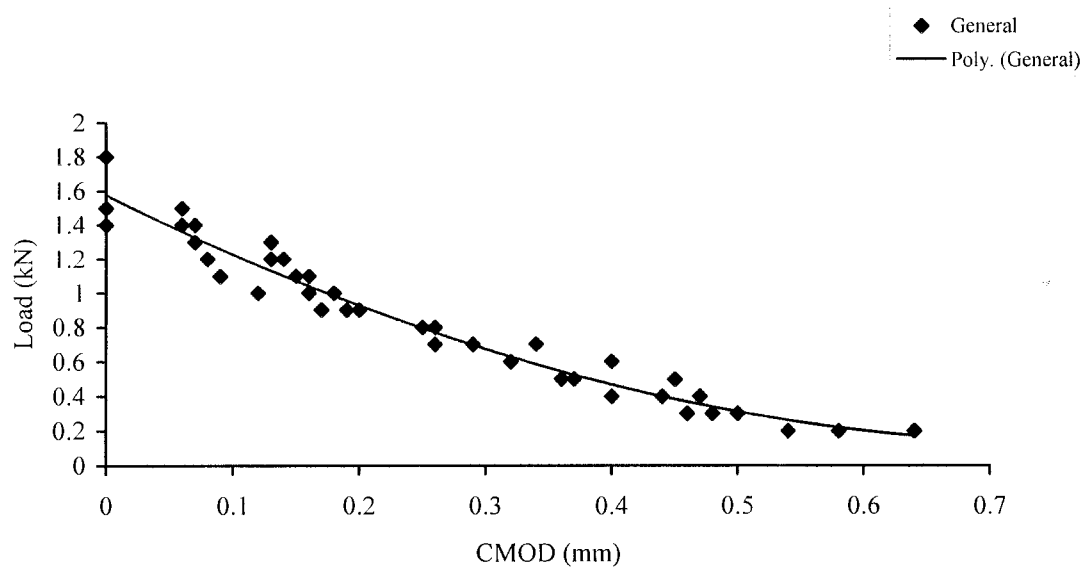


Fig.11: General curve for HSC with $w/b = 0.375$.

CONCLUSIONS

The high strength concrete exhibits higher compressive strength at increased quantity of silica fume at about 0.32 water-binder ratio. An optimum combination of w/b ratio and the quantity of silica fume seem to exist, which is difficult to conclude in these limited experiments. Further experiments are planned to verify the behavior. The fracture energy decreases as the water-binder ratio increases with 10 % and 15 % silica fume contents, while with 20 % silica fume, the fracture energy increases. Fracture energy and the corresponding characteristic length of high strength concrete slightly increases as the compressive strength increases. However, the characteristic length of concrete decreases as the compressive strength increases. It has been generally observed that the ascending portion of the load-CMOD curve is linear up to about 90 percent of the peak load and it gradually drops off in the softening region. From the knowledge of the variation of load versus CMOD, the ductility of concrete, indicated by the extension of tail end of the softening curve increases as the strength of concrete decreases.

References

1. ACI Committee 363, "State-of-the-art Report on High-Strength Concrete", ACI Materials Journal, 1984, pp.48.
2. Bazant, Z.P., and Oh, B.H., "Crack Band Theory for Fracture of Concrete", Materials and Structures, Vol.16, No.93, 1983, pp.155-177.
3. Barr, B.I.G., Nasso, E.B.D., and Weiss, V.J., "Effect of Specimen and Aggregate Sizes upon the Fracture Characteristics of Concrete", Journal of Cement Composites and Light Weight Concrete", V.8, N.2, May 1986, pp.109-119.
4. Barr, B.I.G., and Hasso, E.B.D., "Fracture Toughness Testing by Means of the SECRBB Test Specimen", Journal of Cement Composites and light weight Concrete, V.8, N.1, February 1986, pp.03- 09.
5. Giaccio, G., Rocco, C., and Zerbino, R., "The Fracture Energy of High Strength Concretes", Materials and Structures, V.26, 1993, pp.381- 386.
6. Hillerborg, A., Modeer, M., and Petersson, P.E., "Analysis of Crack Formation and Crack Growth in Concrete by Means of Fracture Mechanics and Finite Elements", Cement and Concrete Research, V.6, 1976, pp.773-782.
7. Hillerborg, A.A., "Analysis of One Single Crack", Fracture Mechanics of Concrete edited by F.H. Wittmann, Elsevier Science Publishers, 1983, pp.223-249.

8. Hillerborg, A., "The theoretical basis of a method to determine the fracture energy G_f of concrete", *Materials and Structures*, Vol. 18, No. 106, 1985, pp.291-296.
9. Hillerborg, A.A., "Results of Three Comparative Test Series for Determining the Fracture Energy G_f of Concrete", *Materials and Structures*, V.18, No.107, 1985, pp.33-39.
10. Kim, J.K., Lee, C.S., Park, C.K., and Eo, S.H., "The Fracture Characteristics of Crushed Lime Stone Sand Concrete", *Cement and Concrete Research*, V.27, N.11, 1997, pp.1719-1729.
11. Nallathambi, P., Karihaloo, B.L., and Haeton, B.S., "Effect of Specimen and Crack Sizes, Water/Cement Ratio and Coarse Aggregate Texture up on Fracture Toughness of Concrete", *Magazine of Concrete Research*, Vol. 36, No. 129, 1984, pp.227-236.
12. Petersson, P.E., "Fracture Energy of Concrete: Method of Determination", *Cement and Concrete Research*, V.10, 1980, pp.79-89.
13. Petersson, P.E., "Fracture Energy of Concrete: Practical Performance and Experimental Results", *Cement and Concrete Research*, V.10, 1980, pp.91-101.
14. Philips, D.V., and Binsheng, Z., "Direct Tension Tests on Notched and Un-notched Plain Concrete Specimens", *Magazine of Concrete Research*, Vol. 45, No. 162, 1993, pp. 25-35.
15. Rao, G.A., and Raghu Prasad, B.K., "Size effect and fracture properties of HPC", *Proceedings of the 14th Engineering Mechanics International conference (ASCE)*, Texas, Austin, May 21-24, 2000.
16. Rao, G.A. and Raghu Prasad, B.K., "Elastic and Mechanical Properties and their Relationships in HSC", *Indian Concrete Journal* (submitted for publication), 2000.
17. Rao, G.A., and Raghu Prasad, B.K., "Fracture Energy and Softening Behavior of HSC", *Cement and Concrete Research* (Submitted for publication), 2000.
18. RILEM DRAFT RECOMMENDATION, "50-FMC Committee Fracture Mechanics of Concrete", *Materials and Structures*, Vol.18, No.106, 1985, pp. 285-290.
19. RILEM, "Fracture Mechanics Test Methods for Concrete (FMC 89)", (ed.Shah and Carpentari), Chapman and Hall, 1990.
20. Sabir, B.B., Wild, S., and Asili, M., "On the Tortuosity of the Fracture Surface in Concrete", *Cement and Concrete Research*, V.27, N.5, 1997, pp.785-795.
21. Sabir, B.B., "High-Strength Condensed Silica Fume Concrete", *Magazine of Concrete Research*, Vol. 47, No. 172, 1995, pp. 219-226.
22. Tasdemir, C., Tasdemir, M.A., Lydon, F.D., and Barr, B.I.G., "Effects of Silica Fume and Aggregate Size on the Brittleness of Concrete", *Cement and Concrete Research*, Vol. 26, No. 1, 1996, pp.63-68.
23. Tasdemir, C., Tasdemir, M.A., Mills, N., Barr, B.I.G., and Lydon, F.D., "Combined Effects of Silica Fume, Aggregate Type, and Size on Postpeak Response of Concrete in Bending", *ACI Materials Journal*, Vol. 96, No. 1, January-February, 1999, pp.74-83.
24. Walsh, P.F., "Fracture of Plain Concrete", *The Indian Concrete Journal*, V.46, No.11, 1972, pp.469-476.
25. Wittmann, F.H., Rokugo, K., Brushwiler, E., Mihashi, H., and Simonin, P., "Fracture Energy and Strain Softening of Concrete as Determined by means of Compact Tension Specimens", *Materials and Structures*, Vol. 21, 1988, pp. 21-32.
26. Yogendran, Y., Langan, B.W., Haque, M.N., and Ward, M.A., "Silica Fume in High-Strength Concrete", *ACI Materials Journal*, V.84, 1987, pp. 124-129.
27. Zhou, F.P., Barr, B.I.G., and Lydon, F.D., "Fracture Properties of High Strength Concrete with Varying Silica Fume Content and Aggregates", *Cement and Concrete Research*, V.25, N.3, 1995, pp.543-552.